

# Guidance, Navigation & Control on-board architecture for Mars Sample Return Rendezvous & Capture

Alexandre Falcoz<sup>(1)</sup>, Pierre Blanc-Paques<sup>(1)</sup>, Keyvan Kanani<sup>(1)</sup>  
Jérémy Lesprier<sup>(1)</sup>, Xavier Manuel-Juanpere<sup>(1)</sup>, Benjamin Charbaut<sup>(1)</sup>, Sophie Narbonne<sup>(1)</sup>  
Leila Lorenzoni<sup>(2)</sup>, Paul Duteis<sup>(2)</sup>, Christoph Steiger<sup>(3)</sup>

(1) Airbus Defence and Space SAS, 31 Rue des Cosmonautes, 31400 Toulouse, France

(2) European Space Agency – ESTEC, Noordwijk, The Netherlands

(3) European Space Agency – ESOC, Darmstadt, Germany

## ABSTRACT

Mars Sample Return (MSR) is a key NASA/ESA exploration mission to bring the first samples of Mars material back to Earth for scientist in-depth analysis. Once collected by Perseverance and injected into Mars's orbit by the Mars Ascent Vehicle (MAV), the Orbiting Samples (OS) will be detected, captured and brought back to Earth safely by the ESA's Earth Return Orbiter (ERO) in the early to mid-2030s. This paper focuses on the Guidance, Navigation and Control (GNC) architecture engineered by Airbus Defence and Space to address the uncooperative rendezvous & capture with the OS. Rendezvous profile incorporates a series of co-elliptical transfers, gates and station keeping points implemented for flight software parameterization, data verification and ground clearance needs to resume the approach. A Narrow Angle Camera designed by Sodern is used as primary sensor for far navigation, then replaced by Jena-Optronik RVS 3000 scanning LiDAR for proximity operations and capture. Orbital control modes are tailored to address rendezvous specificities, then limiting extra-design to a single hybrid wheels/thrusters control mode to compete with stringent capture performances. Development of GNC software is strengthened with hardware in the loop functional verification campaign to be done at DLR's institute on EPOS robotic test facility.

## 1 Navigating against adverse conditions

### 1.1 OS imaging capability

Designing a rendezvous system is a tightly coupled problem with a definite tendency for snowballing complexity. Identifying and prioritizing the key drivers from the plethora of parameters influencing capture success is a crucial step towards a solid GNC design, then limiting development challenges, complex validation and industrial risk. Angle-only navigation is doubtless the key concern to be considered when designing the reference flight trajectory and GNC software. The lack of full states observability requires filtering multiple Line-Of-Sight (LOS) measurements from the navigation camera together with non-gravitational maneuvers to help solving the scale factor paradigm. A target centroiding function (i.e., TgC), hosted in the NAC's FPGA, is used as the primary sensor for far-range navigation. The OS Center-of-brightness is then computed from two successive images and feed to the navigation filter in charge of computing the relative position of the spacecraft Center of Mass (CoM) with respect to the OS. NAC sensor is operating in the visible spectrum, then depriving the navigation from permanent measurement. Even if NAC TgC performance is influenced by many parameters (e.g., detector noises, position of Sun), the exposure time is probably the key element since responsible for collecting sufficient number of photons to ensure OS detection - its tuning is

tricky since tightly coupled with initial in-track separation between OS and ERO. When dealing with faint object like the OS, scarcity of photons disturb the centroid detection property, especially when neighborhood starry sky is brighter or with magnitude close to the OS. As the object apparent brightness decreases with the square of distance, it results that the probability to reliably detect the OS is related to the OS-ERO in-track separation; lower this separation is, higher the probability of detection will be. Eliminating bright objects (e.g., MAV, stars) which could cross the NAC FOV is essential for a reliable OS detection, preceding tracking. By reversing the trajectory profile (i.e., ERO looking behind), MAV detection is excluded by design since floating ahead and below ERO. Therefore, discriminating the OS among stars remains the main concern.

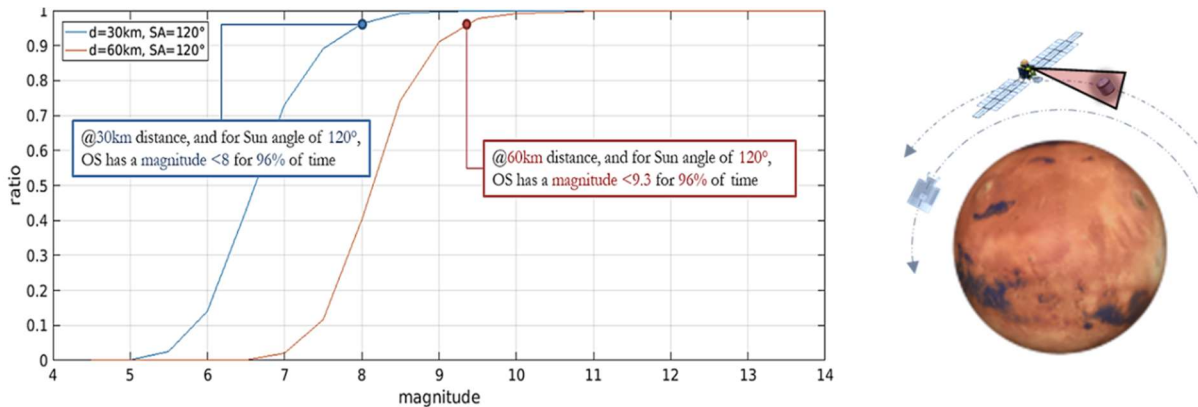


Figure 1. (Left) Preliminary OS magnitude truncated cumulative function depending to distance, for a Sun Angle (SA) of 120°, (Right) flight configuration of ERO

Left part of Figure 1 presents the (truncated) cumulative probability function of the OS magnitude (albedo of 0.5) at 30 km and 60 km of distance. If the OS magnitude is lower than 8 in 96% of time at 30 km, same probability falls down to 40% when 60 km of in-track separation is considered. It results that stars of higher magnitude (up to 9.3) must be considered to unambiguously dissociate the OS from others stars. Figure 2 provides a statistical distribution of stars seen by the NAC as a function of distance. No less than 140 stars are expected to cross the NAC FOV at 30 km against almost 450 at 60 km of distance. This corresponds to 20% and 40% of FOV to be masked<sup>1</sup>, respectively, then directly impacting the time need to robustly detect the OS, i.e. without false alarms then by filtering over further detected samples to remove potential outliers and protons.

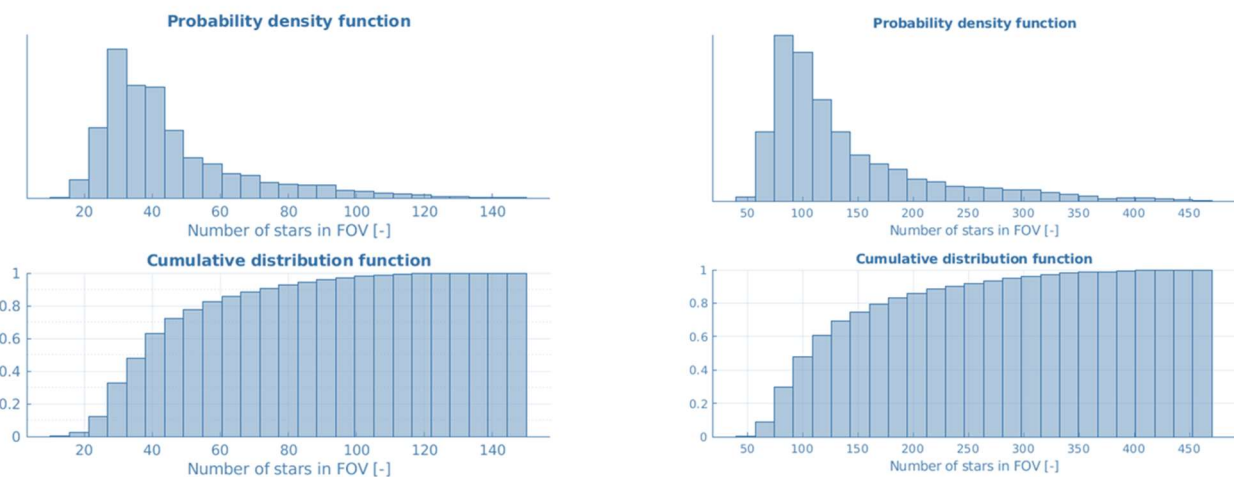


Figure 2. Preliminary distribution of visible stars in the NAV at 30 Km (left) and 60 Km (right)

<sup>1</sup> Fraction of FOV to be masked is not linear with the number of stars. Several stars can be removed with only one mask. Others masks for dead pixels are also considered.

Eliminating stars can be managed either by implementing a catalogue of stars or by considering software parametrization when ERO is delivered at the rendezvous phasing point (HIP). Second option is preferred for obvious numerical concern, then avoiding implementing hundreds of thousands stars on-board. Expected inertial direction of stars to be masked are then computed on-ground and updated to the GNC software, next in charge of automatically compute pixel masks in the NAC imaging frame. Locating HIP at 30 km then offers a good compromise in terms of number of masks, time for initialization and NAC TgC performances compared to further distance.

## 1.2 Compatibility with phasing and communication

Nonetheless, even if 30 km is suited for NAC TgC standpoint, compatibility with phasing accuracy at HIP delivery shall be checked considering *i)* ERO's instantaneous orbit determination errors, *ii)* forecast orbit matching maneuver from the last orbit determination and *iii)* the OS orbit miss-knowledge associated to possible orbits<sup>2</sup>. Assuming that ERO is located on the same orbit than the OS, 30 km behind, it can be seen on Figure 3 that the OS visibility is guaranteed, even considering a long-duration free-floating motion.

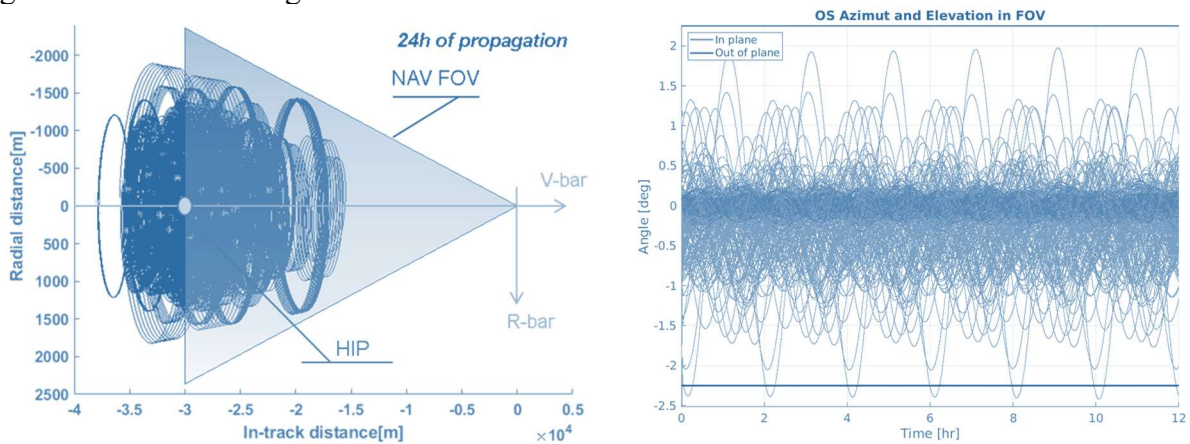


Figure 3. ERO free-floating motion at HIP and OS visibility in the NAV FOV

Because the NAC TgC is operating in the visible spectrum, imaging capacity is restricted to a portion of orbit depending to some parameters, i.e., mainly the NAC Sun exclusion angle ( $\pm 30$  degree), Sun phase angle<sup>3</sup> and  $\beta$ -angle (from 0 to 52 degree of range). Left part of Figure 4 provides the portion of orbit when NAC TgC can be operated for different OS altitude injection.

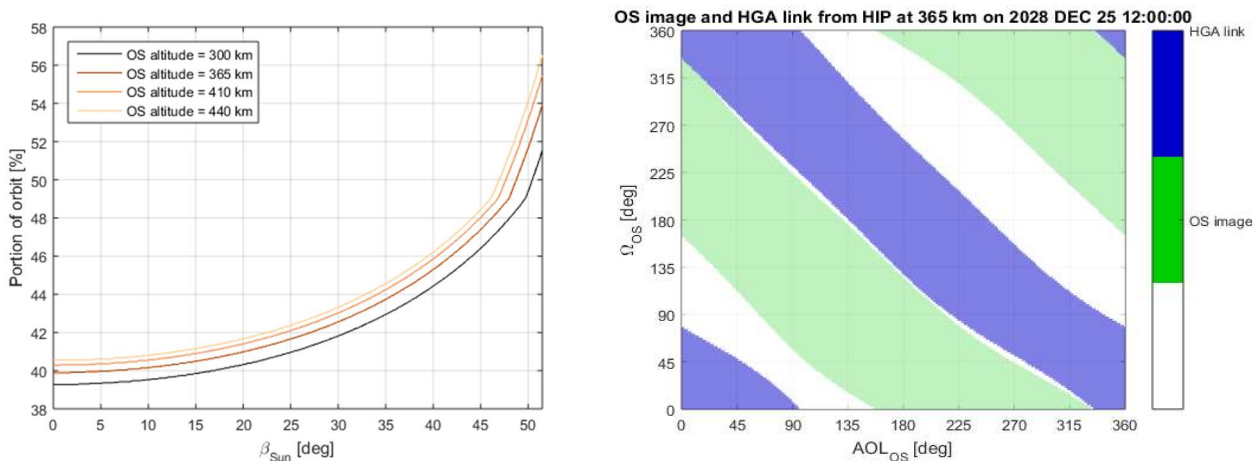


Figure 4: (Left) OS imaging capability, (Right) Imaging and downlink patterns

<sup>2</sup> A set of OS candidate orbits corresponding to the MAV dispersion at OS release must be considered.

<sup>3</sup> NAC TgC is restricted to operate for a Sun phase angle below 120 degree.

Even if the OS imaging capability is marginally improved with the OS injection altitude, OS detectability is limited to 39% of time per revolution; then definitively considered as the strongest design constraint for the design of the trajectory profile and navigation software.

Because antennas link is required for software parametrization and clearance, a readable view of communication slots, together with the imaging phases is key. Two steerable antennas are mounted on ERO. The High Gain Antenna (HGA), steerable in the +Ysc half-space, is mainly used for images downlink. The X-band Medium Gain Antenna (MGA), scanning the -Ysc half space is reserved for Tele-Command (TC) and Housekeeping telemetry. Right part of Figure 4 illustrates both imaging and HGA downlink patterns when ERO is located on the same orbit that the OS, at 30 km of distance looking behind. Imaging phase starts before the downlink capacity meaning that the acquired images can be downlink immediately after acquisition. Reversing the trajectory (looking forward) would be detrimental; the imaging sequence would be followed by a black-out phase leading to the downlink of oldest images on ground and more time to analyze and react.

Overlap capability between imaging and HGA/MGA (i.e., permanent visibility) also depends to the date of the RDV and necessarily influences delay for ground processing, investigation and clearance for resuming the approach. Especially, NAC TgC initialization would require commissioning the centroid function, then cross-checking with native images before acceptance for feeding the data to the navigation filter. Left part of Figure 5 superimposes imaging and communication patterns over one revolution for different dates of RDV. Bold lines correspond to the guaranteed patterns whereas dotted lines refer to the variation of duration as a function of the orbit geometry (i.e., RAAN). It results that: *i*) Imaging windows is guaranteed about 45mn per orbit independently to orbit geometry and date, *ii*) about 70mn of communication coverage is provided cumulating MGA with HGA pattern over one revolution, *iii*) half an orbit of time could be necessary before downlinking the first acquired images in absence of imaging and HGA slots overlap.

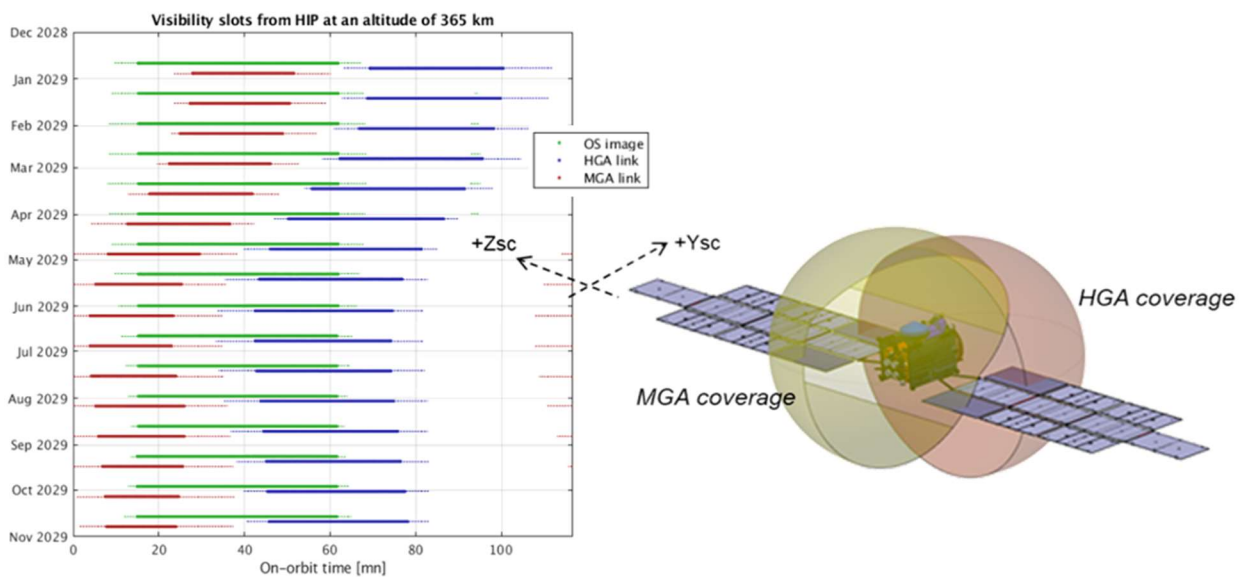


Figure 5: OS imaging capability depending to OS altitude and date

### 1.3 Dealing with a complex Mars's gravity field

Initialization of TgC function requires time, then preventing the navigation filter from measurement. Under considerations of long observation gap, measurement non-linearity, partial observability and the strong anomaly of Mars' gravity field, the navigation filter shall be design to preserve consistency all during NAC TgC initialization and other outage periods while being accurate enough to predict

the expected position of the LOS when measurement is recovered to limit the number of masks once navigation and TgC are coupled.

Plenty of candidate propagation models can be used to derive the relative dynamics motion with multitude range of applicability as a function of in-track separation between objects, orbit eccentricity and the type of perturbations to be modelled (see [1], [2], [3] among others). However, superimposing ERO ground-trace on the GEODIC highlights strong perturbation of the gravity field especially over the Mons Olympus and the nearby mountains regions (see Figure 6). Since the relative in-track position knowledge is tightly coupled with gravity harmonics, the only way to limit secular growth of the differential of orbital elements, then limiting in-track relative error over time requires implementing a sufficiently accurate propagation model.

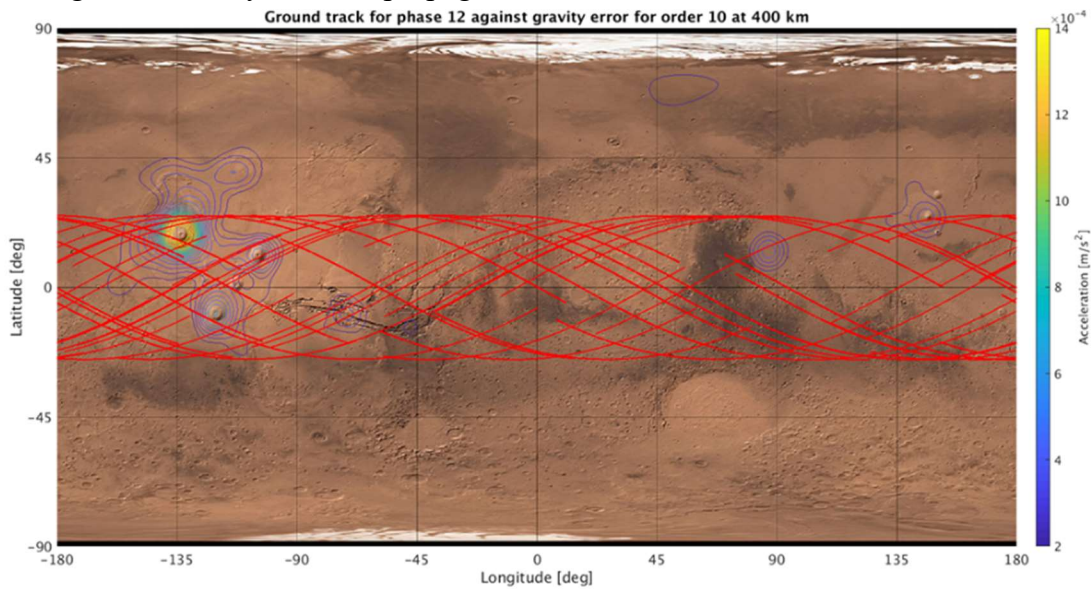


Figure 6: Mars normalized gravitational perturbation map @400Km over ERO ground-trace

MSR-ERO navigation filter is designed to address main of the above listed operational concerns. It is suited to operate with asynchronous data while managing two types of sensors then covering the entire flight envelope, i.e. LOS measurement computed by the NAC TgC for far navigation and 3D relative position when the LiDAR is operated for proximity operations and final translation. As an example, Figure 7 illustrates the error on the relative states all along the trajectory; This latter steadily decreasing with time.

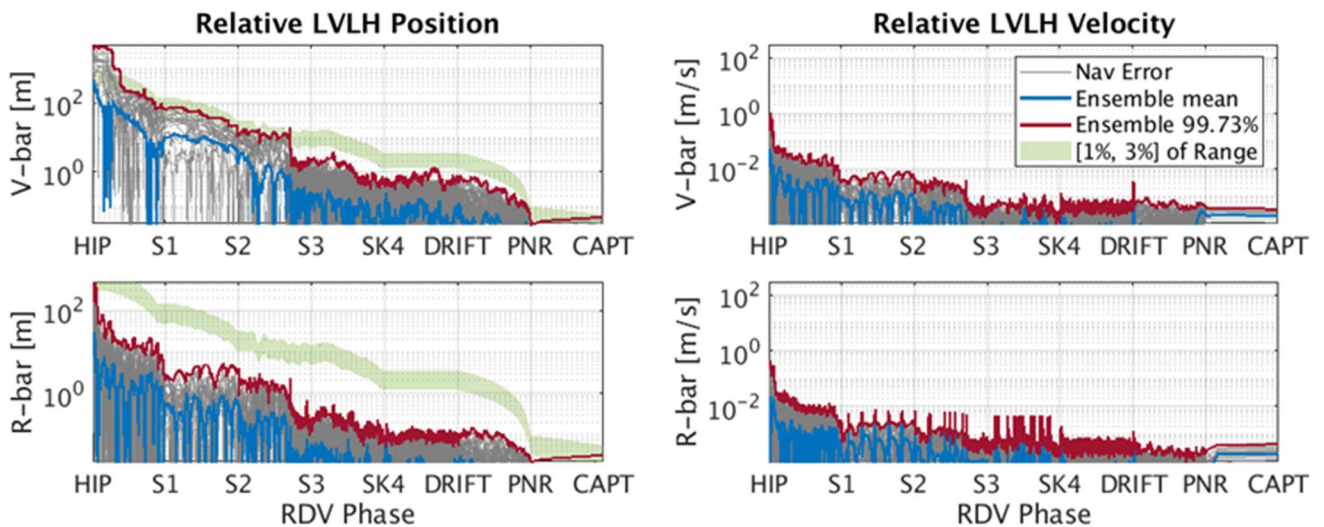


Figure 7: Relative navigation performance along the reference flight trajectory.

## 2 Rendezvous trajectory mission concept

The rendezvous mission profile is defined from the Homing Interface Point (HIP) located on the same orbit than the OS 30 Km forward (ERO looking behind) up to the so-called Point of Non-Return (PNR). This latter, positioned 1.2m rearward the OS, is defined as the ultimate point after which an emergency braking before collision is no longer possible regarding on-board propulsion authority – All the on-board resources for the execution of any reconfiguration actions are then disabled until the capture is achieved and confirmed by the NASA’s Capture, Containment, and Return System (CCRS). Reference trajectory consists of several legs as illustrated on Figure 8, i.e. 1) RDV initialization phase from HIP to S0, 2) Pre-Hopping from S0 to S1 (5Km), 3) Hopping leg from S1 to S2 (1 Km), 4) Closing from S2 to S3 (400m), 5) positioning from S3 to SK4 (60m) and 6) the final translation from SK4 to S5 (i.e., the ultimate position control point).

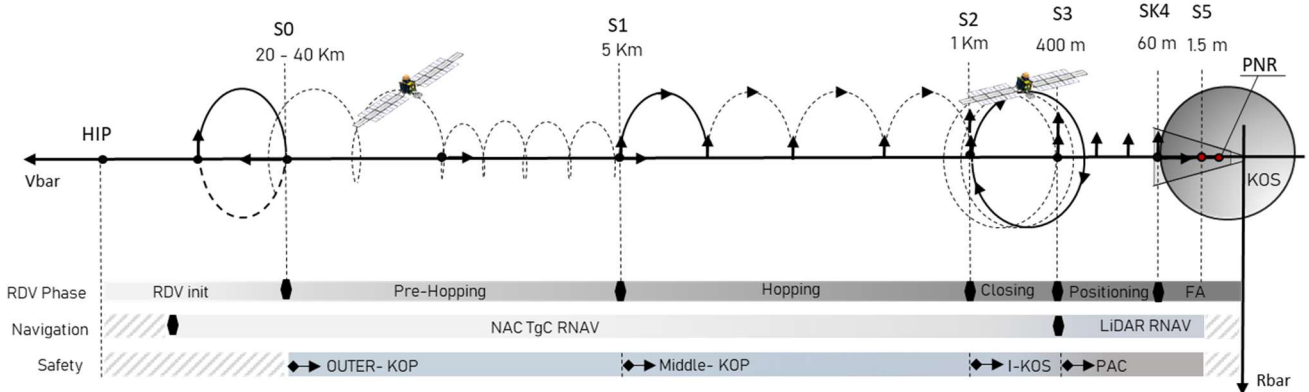


Figure 8. Rendezvous trajectory reference profile

Four Hold points (i.e., S0/S1/S2/S3) are introduced to provide ground opportunities for checks and operations. Hold points are nominally located considering a differential of semi-major axis with respect to the OS, then guaranteeing long-term protection with respect to collision once the braking boost realized. From operation standpoint, Hold Points are used for verification and update of some GMSW flight parameters made applicable for the next trajectory leg (e.g., number of manoeuvring arcs, Keep-Out-Plane value, FDIR thresholds, contingency responses...). Then, in absence of ground clearance, ERO is not allowed to leave its current Hold Point then passively preventing against risk of collision. When passive safety properties are no longer feasible, a collision avoidance manoeuvre (CAM) is armed, both on the nominal and safe-guard On-Board Computers.

### 2.1 Initialization on-board navigation

At HIP, ERO is operated in Normal Mode (NM) pointing towards the expected position of the OS based on a pre-programmed attitude pointing profile (i.e., Nadir Biased Pointing mode profile). The relative navigation filter is automatically initialized in a “pure propagation” mode (no measurement) and the NAC sensor is operated in centroiding mode over its full operating FOV (i.e., 4.5 deg). A set of masks is autonomously computed by the GMSW. The acquired images and the Line-of-Sight computed by the NAC SW are send to ground for verification and to get authorization for processing in the navigation filter. Once LOS convergence is achieved, expectation of the OS position in the FOV is used to reduce the NAC operating FOV and then limiting number of masks. Permutation from the NBP to Target Pointing Mode (TPM) is then commanded by the RDV scheduler.

Then, position of the OS in the NAC FOV is expected to be, and to remain, on the NAC center. According to this optical chain initialization and phasing dispersion, ERO is expected to be located

in the range of 20-40Km rearward the OS at the so-called S0 fictitious gate after free-floating propagation from HIP.

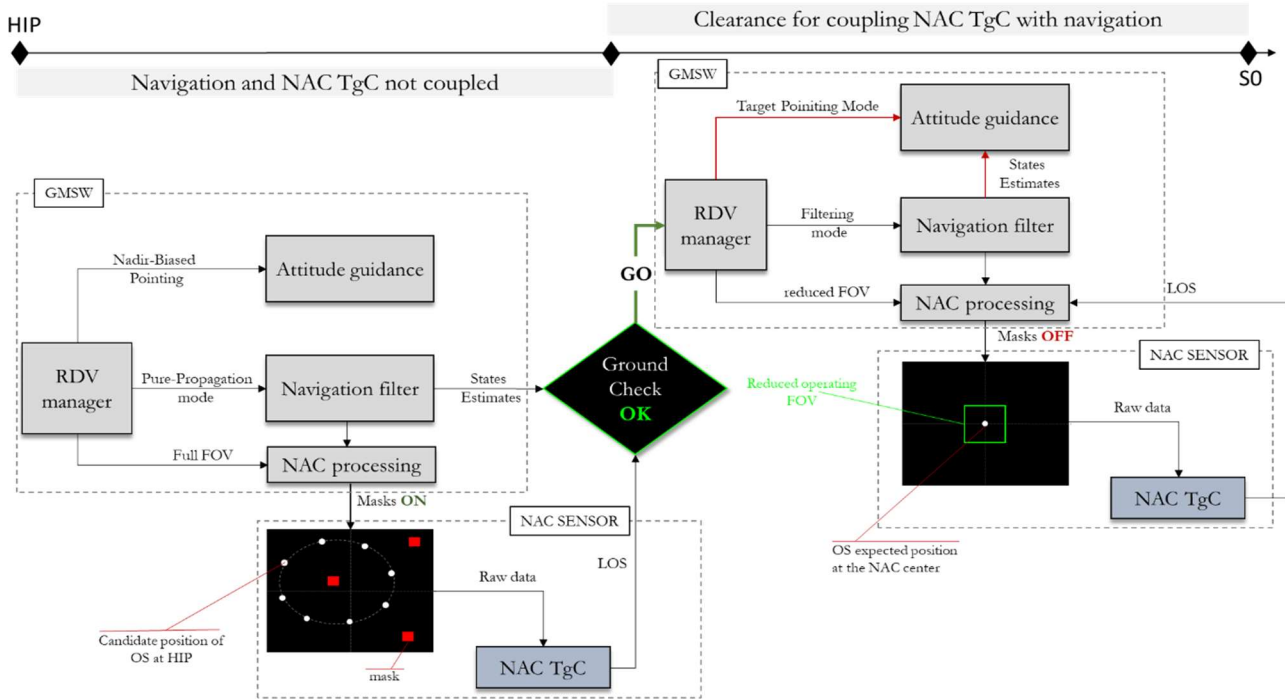


Figure 9. Optical chain initialization sequence

Once clearance for using the NAC TgC in closed-loop with the navigation filter has been received from ground, an observability manoeuvre is autonomously executed by the GMSW in the form of a pre-programmed radial DV. Full-state convergence is then obtained, allowing resuming the approach safely.

## 2.2 Pre-Hopping, Hopping and closing legs

Pre-Hopping leg is defined between S0 gate and S1 Hold Point. S1 is nominally located 5 km forward the OS (along +V-bar axis) with a small differential of semi-major axis ( $\Delta R\text{-bar} \neq 0$ ) to ensure a safe distancing motion in free-floating mode. Shape of Pre-Hopping leg can take different forms according to the safety management policy and mass budget. In our case, a tangential transfer along V-bar is chosen, then consisting in “pushing” ERO on a forward drifting orbit based on a tangential impulse. Forward motion is then initiated at S0 (Go ahead) and autonomously stopped at S1. An intermediate corrective boost is introduced both to improve accuracy at arrival while limiting mean chaser drift velocity. Since any long term un-controlled drift or failure could lead to risk of collision, CAM is armed before leaving S0.

Hopping leg is next defined from S1 (Go ahead) to S2 Hold Point. S2 is nominally located 1 km forward the OS along +V-bar. Safety property of this leg is passively addressed by the execution of a finite number of radial boosts automatically computed and executed by the GMSW; boosts being commanded when the estimated target’s sma is crossed. ERO motion is automatically stopped at S2 on a fictitious point not strictly located on V-bar but on a co-elliptic orbit sized to cover effects of boost braking failure, orbit pollution (induced by SAM execution) and  $3\sigma$  dispersions related to the navigation and closed-loop performances.

Closing phase starts at S2 Hold Point (GO Ahead) up to S3 nominally located at 400 m rearward the OS. This leg is introduced to passively manage the transition from NAC to LiDAR. The closing maneuver consists of single radial boost size to reach a fictitious targeted point (S3.b) positioned

sufficiently closer to the OS in order to guarantee that *i)* ERO will follow a retrograde free-floating mean motion w.r.t the OS, *ii)* ERO will never enter in the I-KOS even in case of thruster issue during the departure boost execution issue and *iii)* ERO motion could be nominally stopped on V-bar axis at S3 after few revolutions.

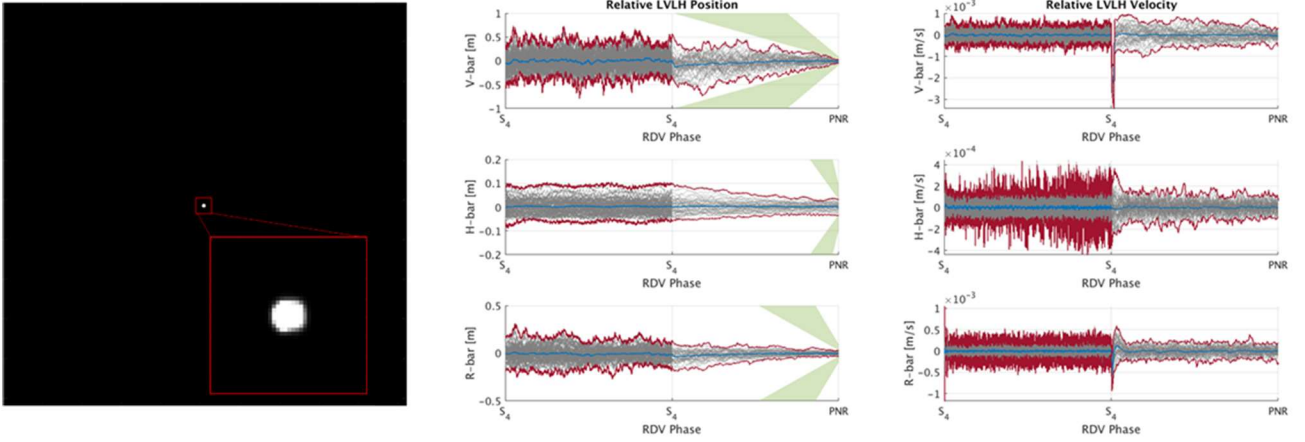


Figure 10. (Left) Simulated images of NAC at 400m with  $60^\circ$  Sun phase angle. (Right) Navigation performances during the terminal leg

All during the closing leg, ERO will navigate in NM in target pointing mode (TPM) based on LOS TgC navigation mode. No intermediate corrective maneuvers is considered to limit risk of dynamical failure and degradation of pointing stability performance which may degrade the LiDAR detection & tracking properties<sup>4</sup>. GO ahead for departure is given by ground and a first fly-around motion is consider to allow ground verification of LiDAR first acquisitions. Without ground counter-order (No Go), fly-around motion is automatically stopped at the second pass. As for S2, S3 targeted is located with sufficient differential of semi-major axis to ensure that ERO will passively remain out of the KOS. Smooth sensor transition is next operated at S3; ERO still flying in NM. For illustration, left part of Figure 10 presents the OS seen by the NAC at S3 whereas the right part presents the estimation errors on the relative states during the LiDAR phase.

### 2.3 Positioning and final approach

Positioning leg starts at S3 Hold point and consists in locating ERO at the Station Keeping Point SK4 60m behind the OS along the V-bar axis. Transfer is executed with two radial impulses executed in NM and starts once the CAM has been armed and Go Ahead received. Transition from NM to Attitude Position Control Mode (APCM) is automatically operated by the GMSW at SK4. SK4 point is the ultimate stable station keeping point for ground-assisted verification before initiating the final approach. ERO flight configuration is then prepared for capture, (e.g., sensors and closed-loop performances checks w.r.t control box, control and monitoring functions parametrization, CAM strategy, control dead zone, wheels sanity checks like friction torque, kinetic momentum provision, parameterization of disabling mechanisms from PNR to capture confirmation from CCRS TC, etc.). Final approach consists of a straight-line trajectory defined in the LVLH frame. A constant acceleration profile is commanded to reach the targeted velocity (between 2 and 5 cm/s). ERO is pre-positioned to align CCRS boresight with the OS geometrical center for the compensation of the orbital drift motion during the final floating duration, i.e. from PNR to capture. Position control is disabled when the estimated position of ERO reaches the targeted S5 position but CAM execution capability

<sup>4</sup> Note that periodic detection & tracking and loss of tracking are expected to occur due to the LiDAR operating domain



remains active up to PNR after which FDIR capability is disabled. Attitude control is kept active up to capture.

## 2.4 Performance evaluation

Complete trajectory is now designed, fully implemented in Airbus’s FAME environment (Functional Avionics Multi-purpose Environment) integrating dynamics of both the OS (target) and the ERO (chaser), the full nominal GNC modules and functions, and performance models of actuators (thrusters and RW), sensors (mainly NAC, LiDAR, GSE) with their related image processing performance model and operating constraints (e.g., phase angle, Eclipse, Sun exclusion angle, min/max operating domain, outlier), orbit propagator, disturbances (e.g., gravity gradient due to Mars, drag and solar radiation pressure) and Sun ephemeris. The dynamical model of the ERO is a coupled 6-DoF model taking into account the appendages’ flexible modes, slosh dynamics and plumes effects. Figure 11 provides a condensed view of results, then demonstrating applicability of the mission profile fulfilling the stringent capture requirement (i.e., less than  $\pm 10$  cm  $3\sigma$  cross-track/radial errors).

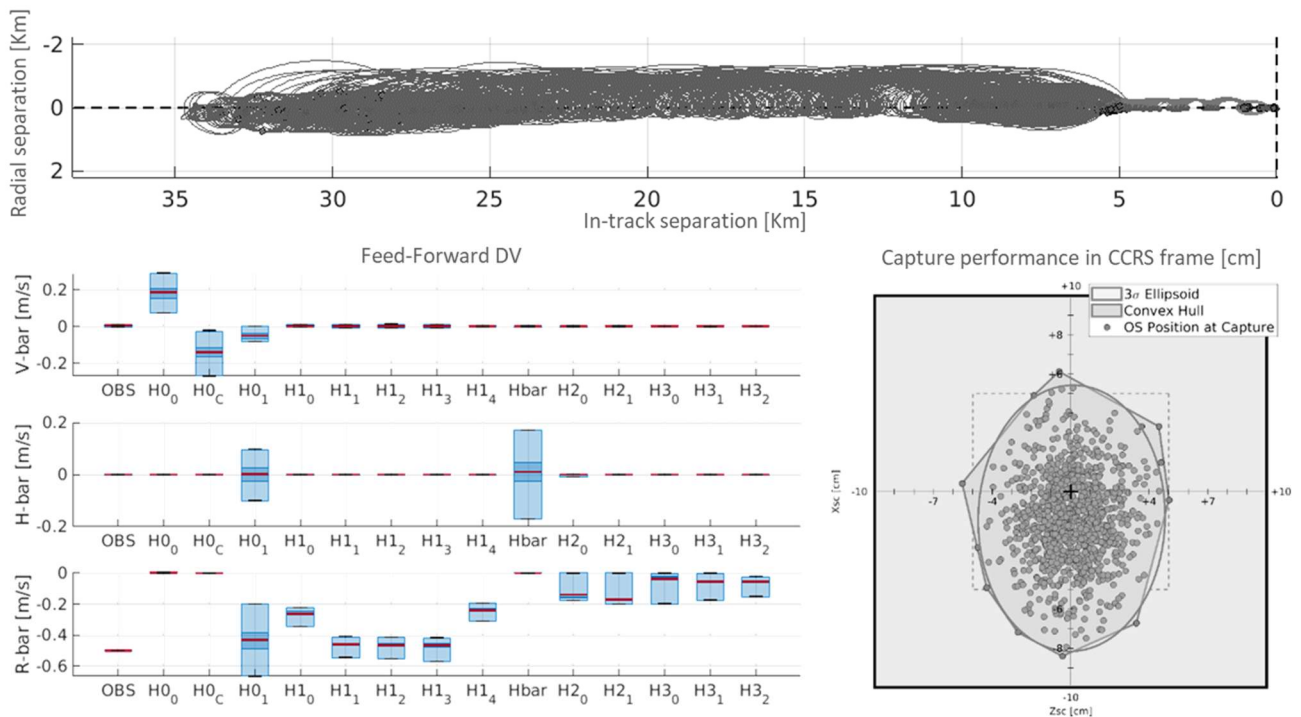


Figure 11. (Top) Family of trajectories from HIP to capture, (bottom left): boost maneuvering plan, (bottom right): performances at capture.

## 3 A fault-tolerant avionic architecture

GNC MCL functions (GMSW) required for the execution of RDV are hosted in 2 cold-redunded (x2) OSCAR mk4 On-Board Computer (OBC1) with LEON3. FDIR functions as well as the Mode Vehicle Manager are also hosted in OBC1 GMSW.

When the need for arming a retreat or collision avoidance manoeuvre, OBC1 “operating status” is monitored by a dedicated Safe-Guard On-Board Computer (OBC2). This latter is in charge of executing the emergency manoeuvre in the case where the OBC1 is suspected to be failed (e.g., heartbeat, watchdog) or when a CAM is commanded by OBC1 CSW after a L4-type reconfiguration action. OBC2 is connected to its proper resources (MilBus2 1553, PCDU, RIU), GNC sensors (STR3, IMU3), actuators (THR-B) and the required processing functions (CAT-A MAM-SW).

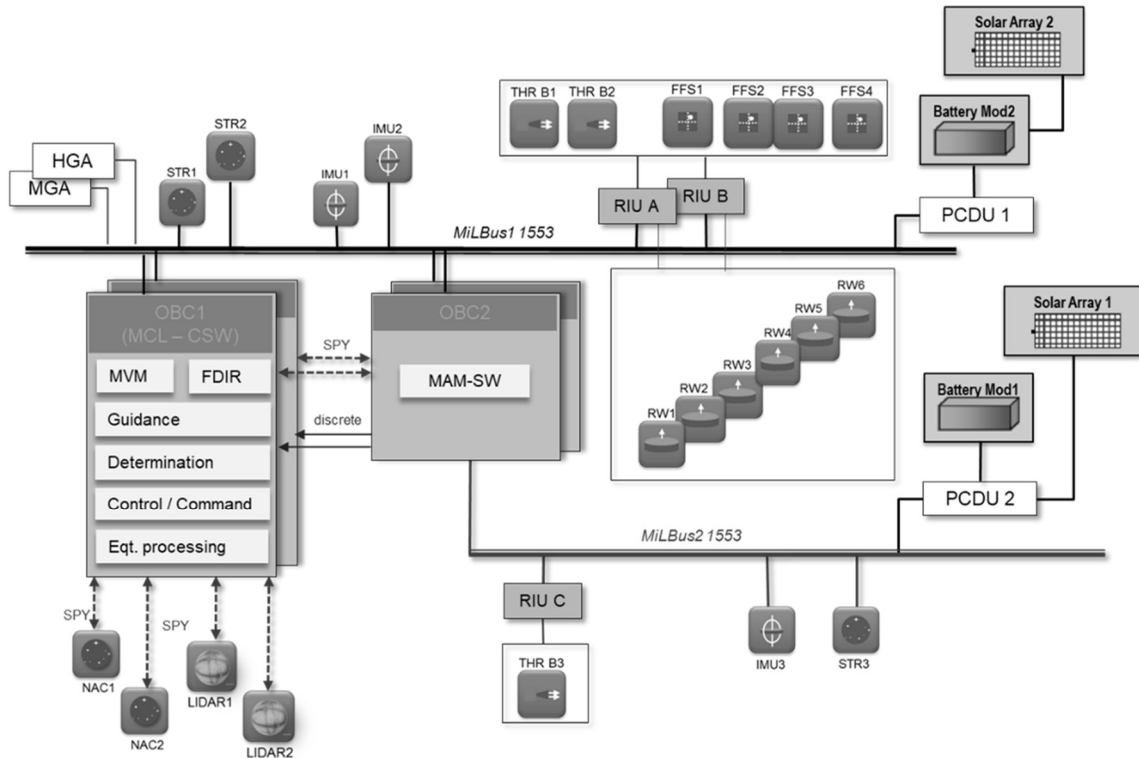


Figure 12: Simplified on-board electrical architecture

### 3.1 Optimising the thruster geometry for capture

Three branches of ArianeGroup thruster (LEROS 10) are considered. Branch n°1 is nominally used during the GNC function whereas Branch n°3 is reserved for the execution of the CAM manoeuvre; Branch n°2 being only composed of a set of 4 THR usable for EAM. Thruster's geometry is optimized to ensure simultaneous multi-axis pure force capacity during the rendezvous final approach and 3-axis pure torque capacity to address specific CPS-based attitude control modes (i.e., C-SAM, OCM, EAM). Especially, thruster positions and tilts have been optimized to limit along-track parasite fires during radial (R-bar) and cross-track (H-bar) relative position control. This last consideration is a major accommodation driver to limit plumes impingement on the OS during the final translation while avoiding implementing a stiff in-track position control which could lead to undesirable excitation effects on ERO bending modes and negative impacts at capture.

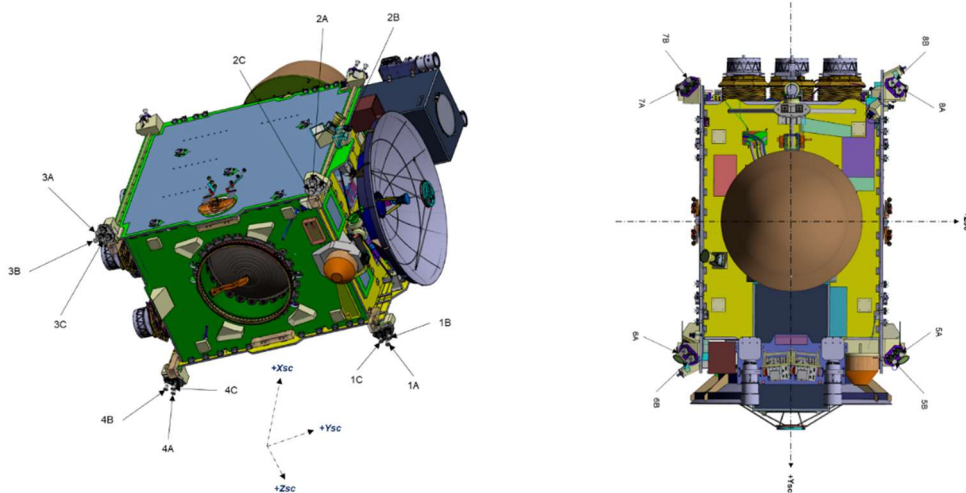


Figure 13: Thruster accommodation with main thrust direction constraints

Thrust efficiency is also part of consideration and maximized in the “most demanding”  $DV$  direction while preventing for risk of Propellant Management Device (PMD) defusing related to the tank filling ratio. Since “Long-term” negative and lateral thrusts with respect to the tanks lengthwise have to be limited, to remain in the PMD capacity, thrust efficiency and usage is maximized towards S/C +X-axis which also correspond to the direction of the most consuming boosts. Thrust efficiency is finally optimized keeping risk of clashes with other equipment under considerations. Especially, solar arrays, the voluminous High Gain antenna as well as the reserved volume for CCRS implementation on the S/C +X wall harshly restrict the possibility of implementation.

### 3.2 Navigation and attitude sensors

Three Jena-Optronik Astro APS star trackers and three IMU Astrix 1090 are considered to provide inertial attitude of the S/C. Two IMUs and two STR are connected to OBC1 and the others sensors are reserved for OBC2. Note that the capability to connect any (inertial) sensors to the two OBC is kept. LiDAR1 and LiDAR2 are both connected to OBC1 via Space-Wire communication protocol. There are operated in warm redundancy meaning that LiDAR 1 is nominally used in the GNC functions whereas LiDAR2 is used in “open-loop” for consistency check of the LiDAR1 (i.e. only one LiDAR measurement is processed by the navigation filter). LiDAR directly provides LOS and range measurement related to each point shooting the OS as well as the output of the process points cloud, i.e., Barycentring algorithm. Measurements are either given in terms of 3D relative distance between the OS geometrical pinged surface and the LiDAR reference frame or in terms of LOS/range. NAC1 and NAC2 are also connected to OBC1 via Space-Wire. They are operated in warm redundancy, then both initialized in TgC mode at HIP before departure. In case of failure of the nominal NAC, a retry before switch-over policy is considered.

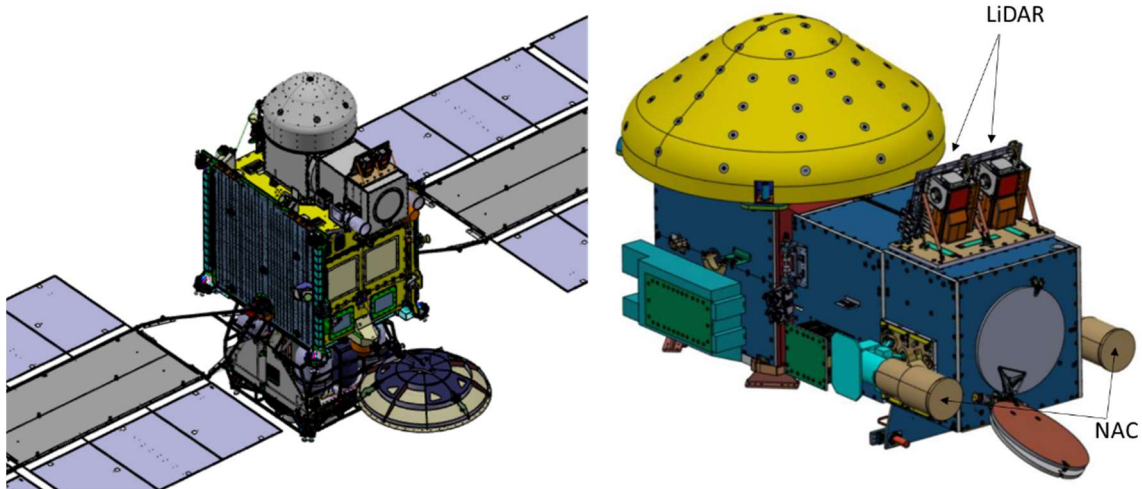


Figure 14. NAC and LiDAR layout on ERO

### 3.3 A dedicated mode for final approach

APCM is the main mode used from SK4 to capture designed to perform Lidar-based Relative Station Keeping and 6 dof controlled straight-line forced trajectory. Its architecture is designed to maximize closed-loop performance for capture hybridizing RW for attitude control (i.e., cluster of 6 reaction wheels - RSI 100-220/60 from RCD) and thrusters for pure-force translational control. Attitude in the S/C body frame is controlled to fit with the estimated LVLH frame. The attitude error between the body CoM and the estimated LVLH frame is then computed by the guidance function thanks to the navigation filters data (i.e. estimated LVLH position) and compared to gyro-stellar estimates. Angular rate motion required to track the estimated LVLH frame is also computed thanks to the estimated

orbital mean motion before comparison with GSE estimate. Attitude and angular rate errors are then feed to the attitude controller for the computation of the control torques to be executed by the cluster of reaction wheels. The relative position between the OS CoM and the S/C CoM computed by the navigation filter is projected in the CCRS capture plan to align the CCRS capture axis thanks to the skew matrix of the estimated vector OC (distance from ERO CoM to CCRS capture centre); the kinematic coupling between the S/C attitude and the position is then perfectly addressed. APCM guidance function is designed to deal with Relative Station Keeping or Straight Line motion. This is managed by adapting the targeted set point in input of the guidance function. Either a fixed SK is considered or a straight line motion is computed - In the latter case, a reference feed-forward acceleration motion is computed in addition to the velocity trajectory profile. Trajectory profile is judiciously adapted, then avoiding over-stress on thrusters firing on the OS.

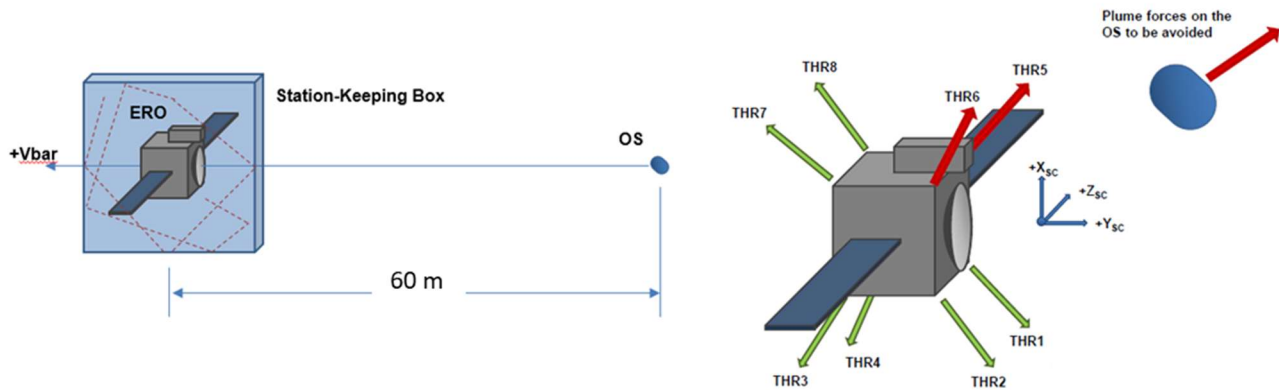


Figure 15. (Left) station keeping box and plume avoidance strategy (right).

Position and attitude controllers are tuned based on robust control methods to simultaneously address control performance and robustness in one shot. A multi-model approach based on a discretised set of plant dynamics is used instead of considering a  $\mu$ -based approach. Main difference rely on the capability to select for each optimisation criteria a set of plant dynamics to be constrained instead of the overall family. The optimisation problem to be solved consists of a diagonal encapsulation of  $H_\infty$  criteria limiting the undesirable off diagonal effects and the conservatism of the solution.

### 3.4 Concluding remarks

In this paper, the GNC architecture to address MSR-ERO rendezvous mission phase has been briefly presented. Design feasibility has been fully demonstrated, now under Phase C/D development. Crucial validation steps will start soon, especially considering hardware-in-the-loop functional verification campaign at DLR's institute to simulate the last 25 meters of the RDV with real HW unit (LiDAR EM). Execution of the Flight Operational Procedure (FOP), HW/SW integration tests, ground-assisted operations, closed-loop reference test cases will be executed on AVM (Avionics Validation Model). More specially, closed-loop reference cases will be replayed to check consistency of both NAC and LiDAR Core Functional Models (CFM) retained for design, compared with real equipment. For the NAC, closed-loop trajectory (real states) from FAME will be replayed inside a dedicated NAC RDV simulator to verify that NAC TgC is well working consistently with CFM implementation. For the LiDAR, a reduced set of trajectory corresponding to the 25 last meters of the final approach will be defined and analysed under FAME environment. This set of trajectory will be executed on EPOS facility to check consistency between the obtained closed-loop performances w.r.t to FAME outputs. NAC and LiDAR stimulators (i.e., NACOS and LiDES, respectively) will be connected to AVM for the stimulation of NAC and LiDAR EM. Surrender renderer will also interfaced to the NACOS for the stimulation of images

#### 4 REFERENCES

- [1] Scharf, D. P., Hadaegh, F. Y., and Ploen, S. R., “A Survey of Spacecraft Formation Flying Guidance and Control (Part 1): Guidance,” Proceedings of the 2003 American Control Conference, IEEE Publ., Piscataway, NJ, 2003, pp. 1733–1739.
- [2] Scharf, D. P., Hadaegh, F. Y., and Ploen, S. R., “A Survey of Spacecraft Formation Flying Guidance and Control (Part 2): Control,” Proceedings of the 2004 American Control Conference, IEEE Publ., Piscataway, NJ, 2004, pp. 2976–2985.
- [3] Alfriend, K. T., and Yan, H., “Evaluation and Comparison of Relative Motion Theories,” Journal of Guidance, Control, and Dynamics, Vol. 28, No. 2, 2005, pp. 254–261.